

Construction of a dimeric form of glutamate dehydrogenase from *Clostridium symbiosum* by site-directed mutagenesis

Alessandra Pasquo^{a,b}, K. Linda Britton^b, Timothy J. Stillman^b, Dave W. Rice^b,
Helmut Cölfen^{c,1}, Stephen E. Harding^c, Roberto Scandurra^a, Paul C. Engel^{b,*}

^a Dipartimento Scienze Biochimiche 'A. Rossi Fanelli', Università La Sapienza di Roma, Piazzale Aldo Moro, 5 00185 Roma, Italy

^b Krebs Institute, Department of Molecular Biology and Biotechnology University of Sheffield, Firth Court, Western Bank, Sheffield S10 2UH, UK

^c Department of Applied Biochemistry and Food Science, University of Nottingham, Sutton Bonington, LE12 5RD, UK

Received 27 July 1995; accepted 25 January 1996

Abstract

By using site-directed mutagenesis, Phe-187, one of the amino-acid residues involved in hydrophobic interaction between the three identical dimers comprising the hexamer of *Clostridium symbiosum* glutamate dehydrogenase (GDH), has been replaced by an aspartic acid residue. Over-expression in *Escherichia coli* led to production of large amounts of a soluble protein which, though devoid of GDH activity, showed the expected subunit M_r on SDS-PAGE, and cross-reacted with an anti-GDH antibody preparation in Western blots. The antibody was used to monitor purification of the inactive protein. F187D GDH showed altered mobility on non-denaturing electrophoresis, consistent with changed size and/or surface charge. Gel filtration on a calibrated column indicated an M_r of $87\,000 \pm 3000$. The mutant enzyme did not bind to the dye column routinely used in preparing wild-type GDH. Nevertheless suspicions of major misfolding were allayed by the results of chemical modification studies: as with wild-type GDH, NAD^+ completely protected one-SH group against modification by DTNB, implying normal coenzyme binding. A significant difference, however, is that in the mutant enzyme both cysteine groups were modified by DTNB, rather than C320 only. The CD spectrum in the far-UV region indicated no major change in secondary structure in the mutant protein. The near-UV CD spectrum, however, was less intense and showed a pronounced Phe contribution, possibly reflecting the changed environment of Phe-199, which would be buried in the hexamer. Sedimentation velocity experiments gave corrected coefficients $s_{20,w}$ of 11.08 S and 5.29 S for the wild-type and mutant proteins. Sedimentation equilibrium gave weight average molar masses $M_{r,app}$ of $280\,000 \pm 5000$ g/mol, consistent with the hexameric structure for the wild-type protein and $135\,000 \pm 3000$ g/mol for F187D. The value for the mutant is intermediate between the values expected for a dimer (98 000) and a trimer (147 000). To investigate the basis of this, sedimentation equilibrium experiments were performed over a range of protein concentrations. $M_{r,app}$ showed a linear dependence on concentration and a value of 108 118 g/mol at infinite dilution. This indicates a rapid equilibrium between dimeric and hexameric forms of the mutant protein with an equilibrium constant of 0.13 l/g. An independent analysis of the radial absorption scans with Microcal Origin software indicated a threefold association constant of 0.11 l/g. Introduction of the F187D mutation thus appears to have been successful in producing a dimeric GDH species. Since this protein is inactive it is possible that activity requires subunit interaction around the 3-fold symmetry axis. On the other hand this mutation may disrupt the structure in a way that cannot be extrapolated to other dimers. This issue can only be resolved by making alternative dimeric mutants.

Keywords: Glutamate dehydrogenase; Subunit interaction; Site-directed mutagenesis; (*C. symbiosum*)

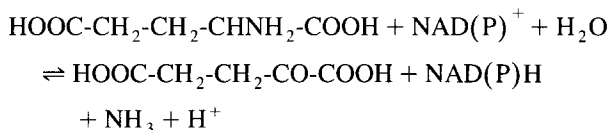
Abbreviations: GDH, glutamate dehydrogenase; Amp, ampicillin; IPTG, isopropyl D-thioglucoopyranoside; DTNB, 5,5'-dithiobis(2-nitrobenzoate).

* Corresponding author. Present address: Department of Biochemistry, University College Dublin, Belfield, Dublin 4, Ireland; Fax: +353 1 2837211.

¹ Present address: Max-Planck-Institute for Colloid and Interface Research, Colloid Chemistry Department, Kantstr. 55, D-14513 Teltow Seehof, Germany.

1. Introduction

Glutamate dehydrogenase (GDH) EC 1.4.1.2–4 catalyses the reversible oxidative deamination of L-glutamate to 2-oxoglutarate and ammonia with nicotinamide nucleotides as coenzyme according to the equation:



This reaction has a key role in nitrogen metabolism and it represents one of the main paths for transforming ammonia into α -amino nitrogen or vice versa.

GDH has been purified and sequenced from various sources. Two main oligomeric classes can be identified: one formed of six identical subunits with an M_r ranging from 47 000 and 55 000 (beef, rat, *Escherichia coli*) and a second class composed of four identical subunits of M_r 115 000 (NAD⁺-dependent GDH of *Neurospora crassa*, *Saccharomyces cerevisiae*) [1,2]. The hexameric GDHs have been the subject of detailed investigations in order to understand the catalytic mechanism [3–6] the coenzyme specificity [7] and allosteric regulation [8,9]. In view of the interest in establishing the importance of the oligomeric structure in determining both activity and allosteric behaviour [10] there have been several attempts to separate the subunits with denaturants either in free solution or after immobilising hexamers on a solid support [11–13]. It has been found that GDHs from *Sulfolobus solfataricus* [14] and from *Bacillus acidocaldarius* [15] elute from a gel filtration column, not as a sharp peak of active enzyme, but as a broad one ranging from 280 kDa to 47 kDa, again focusing attention on the possibility of active GDH species smaller than the hexamer.

The *gdh* gene of *Clostridium symbiosum* has been recently sequenced, cloned and over-expressed in *E. coli* [16]. Crystallographic analysis has revealed the three-dimensional structure of this GDH [17]. The 449 residues comprising the polypeptide chain of a single GDH subunit are organised into two domains separated by a deep cleft (Fig. 1 A). Domain I consists of the N-terminal portion of the polypeptide chain (residues 1–200) and residues 424 to the C-terminus. The second smaller domain, domain II, is assembled from the remaining contiguous stretch of residues from 201 to 423. In all, the structure contains 17 α -helices, 13 β -strands and two short 3_{10} helices, which account in total for 77% of the polypeptide chain.

The oligomeric enzyme is composed of six subunits which assemble into a hexamer with 32 symmetry and can be represented as a squat cylinder (Fig. 1 B). The two domains of each subunit lie virtually on top of one another

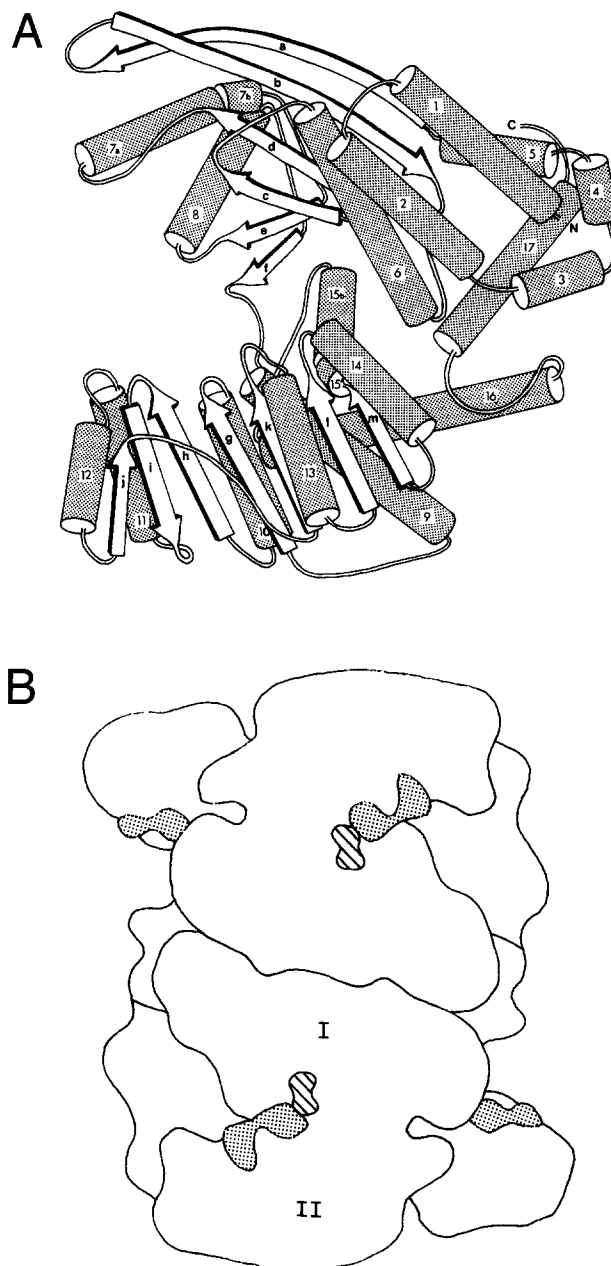


Fig. 1. (A) Schematic diagram of clostridial GDH subunit and hexamer. The model shows the elements of the secondary structure represented by cylinders (α -helices) and arrows (β -sheets). © 1992, John Wiley and Sons, Inc. (B) This model shows how the subunits assemble to form the hexamer with the coenzyme and the substrate bound.

in the direction of the threefold axis. Normal to the direction of this axis the surface of the trimer is not planar, but rather the top of each subunit (as seen in Fig. 1 A) slopes to provide a sawtooth profile, producing a surface which is strongly interlocked as the hexamer forms. Domain I lies closest to the 32 symmetry point and plays a

major role in all intersubunit interactions, the most extensive of which are associated with the trimer. Domain II consists of a predominantly parallel central seven-stranded β -sheet which again is flanked by α -helices. The folding pattern is highly reminiscent of the dinucleotide binding fold, found in many other protein structures [18,19], though with the direction of one of the strands reversed. The active site of the enzyme is located in the cleft between the two domains and an important feature of the catalytic cycle is a dramatic conformational change which closes the cleft and is responsible for the appropriate orientation of the groups involved in the hydride transfer [20]. Thus, each monomer contains both the substrate and the coenzyme binding sites and since the active site does not appear to involve structure elements from other subunits it seems feasible that independent monomers could remain catalytically competent provided that they are able to maintain their tertiary structure and are still capable of undergoing the conformational change required during catalysis without the co-operation of their hexameric partners.

Since alignments for the 25 hexameric GDH sequences published to date show strong homology [21,16], clostridial GDH offers a good framework for understanding structure–function relationships in the GDH family. Analysis of this alignment together with the three-dimensional structure assignment of the *C. symbiosum* enzyme shows that very few residues involved in the interface regions are identical in all species. Of the four such conserved residues, two are involved in the trimer interface (i.e., the interface between dimers to form a trimer), namely residues P87 and G446, leaving the remaining two (V73 and K104) associated with the construction of the dimer. Despite the small number of conserved residues, the trimer interface is extensive, with the residues involved located on many different elements of secondary structure from domain I. These elements include the very end of α_4 ; the very start of β_a ; the loop from the end of β_b up to and including the beginning of β_c ; the loop from the end of α_6 to the start of β_d ; α_{7a} ; the loop between α_{7b} and the start of β_e ; α_8 and the loop to the start of β_f ; a helical loop of the polypeptide chain from 196–200; part of the polypeptide chain including the end of α_{15b} ; the loop to and early part of α_{16} and the end of α_{17} to the C-terminus. One of the important interface interactions is formed by stacking of the side chain of F187 against G86 and the peptide group joining residues 86 and 87 of the symmetry-related subunit (Fig. 2). Another important interaction at the trimer interface includes the interaction of R390 and the extended chain to S392, which in particular serves to bury this side chain which forms hydrogen bond interactions to D158 and S388. A central interaction involves R181 which is buried

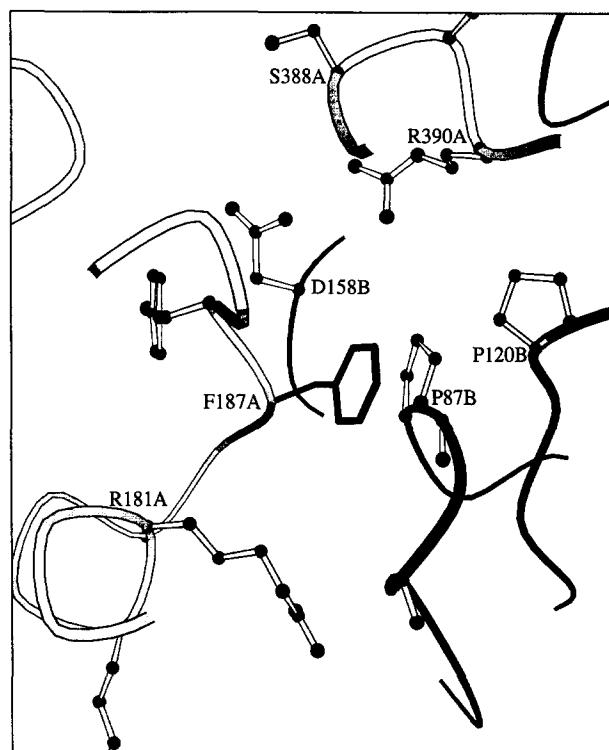


Fig. 2. MolScript model for the residues involved at the trimer interface. The residue mutated in this study is F187. This diagram shows the interaction between subunit A (light shading) and one of its partners in a trimer, subunit B (dark-shaded backbone). The sidechain of F187 (also highlighted in black) from subunit A interacts with P87 and G86 of subunit B.

in this interface forming hydrogen bonds to E55 and Q445. The close approach of the S of M141 to C1 of I447 and a number of hydrophilic interactions, some of which are water-mediated, complete the interface region.

Site-directed mutagenesis has been used to substitute F187 with an aspartic acid in order to introduce a charged residue in a predominantly hydrophobic environment. As predicted, this mutation has led to the production of a dimeric protein. In this paper we report the enzymological and structural characterization of this mutant protein.

2. Materials and methods

2.1. Materials

Restriction enzymes, T4 ligase, T4 polymerase and T4 polynucleotide kinase were purchased from Northumbria Biologicals Limited (UK). U-DNA Mutagenesis Kit was from Boehringer Mannheim (UK). Sequenase 2.0 sequencing kit was from United States Biochemical (USA).

Oligonucleotides used for mutagenesis and gene sequencing were made in the Biomolecular Synthesis Service of the University of Sheffield with an Applied Biosystems 381 DNA synthesiser by Dr A.J.G. Moir and Mr P.E. Brown.

All the chemicals for molecular biology and enzymology were of the highest purity available.

2.2. Bacterial strains and plasmids

The *E. coli* strains used for mutagenesis were: –*Tg1* [Δ lac-proAB, *supE*, *thi1*, *hsd* Δ 5/*F'*traD36, *proA*⁺*B*⁺, *lacI*^q, *lacZ* Δ M15], CJ236 [*dut1*, *ung1*, *thi1*, *relA1*/pCJ105 (*cmr*)]. Bacteriophage M13 mp18 and mp19 were from Boehringer (London). *E. coli* K12 [*thr-1* *fhuA2* *leuB6* *lacY1* *supE44* *gal-6* *gdh-1* *hisG1* *rfbD1* *galP63* Δ (*gltB-F*) 500 *rpsL19* *malT1* *xyl-7* *mtl-2* *argH1* *thi-1*] strain PA340 as well as the expression vector ptac 44 [22] harbouring the gene of glutamate dehydrogenase were kindly provided by Dr J.K. Teller.

2.3. Sub-cloning strategies

Standard protocols [23] were used to subclone the wild-type and the mutated gene in the bacteriophage for mutagenesis and into the expression vector using the *SalI* and *BamHI* restriction sites unless differently stated.

DNA fragments were recovered from agarose gel with GeneClean II Kit (Bio101, USA), or by electroelution and treatment with phenol/chloroform [24].

2.4. Mutagenesis

Site-directed mutagenesis with mismatch primers was carried out with the uracil DNA method [25]. The putative mutants were screened by DNA sequencing with the dideoxy chain termination method [26] using the Deaza Sequenase Kit (United States Biochemicals, USA) either for the ssDNA M13 or dsDNA recombinant ptac44.

2.5. Enzyme preparation

Overnight cultures of *E. coli* transformants were harvested, sonicated in ice-cold conditions and then centrifuged in a Sorvall RC Superspeed refrigerated centrifuge for 30 min at 30 000 $\times g$. Since the mutant enzyme was unable to bind the Remazol red dye column usually employed for purifying the wild-type enzyme, an alternative purification procedure was devised.

The clarified supernatant of the sonicated cells (crude extract) was precipitated with 40% ammonium sulfate at

4°C. The supernatant was adjusted to a final concentration of 60% ammonium sulfate. The pellet was resuspended in 0.1 M phosphate buffer (pH 7) and loaded onto a DEAE Sephadex A-25 (Pharmacia Biotech.) ion-exchange column previously equilibrated with the same buffer. The column was washed exhaustively with the same buffer and A_{280} monitored with a LKB Uvicord II UV detector.

After a further washing with the same buffer supplemented with 0.15 M NaCl, the column was finally eluted with 0.1 M phosphate buffer and 0.25 M NaCl. The desired fractions were pooled and dialysed against phosphate buffer and stored as a precipitate in 65% ammonium sulfate at 4°C. The enzyme was dialysed several times before use against 0.1 M phosphate buffer and clarified by centrifugation. The concentration of the enzyme was calculated on the basis of the absorption coefficient of 1.05 l g⁻¹cm⁻¹ [27].

2.6. Enzyme activity

The activity was monitored spectrophotometrically on a Uvikon 941 Plus (Kontron Instruments) by following the production or the consumption of NADH at 340 nm. The 1 cm path cuvette contained in 1 ml final volume 1 mM NAD⁺ and 40 mM L-glutamate in 0.1 M phosphate buffer (pH 7.0) for the forward reaction, or 0.1 mM NADH, 10 mM 2-oxoglutarate and 50 mM NH₄Cl in the same buffer for the reverse reaction.

2.7. Polyacrylamide-gel electrophoresis

The mutant and wild-type enzymes were screened for level of expression by direct visualisation on polyacrylamide gel after electrophoresis of crude extracts, either native or SDS [28] with a MiniProtean II electrophoretic cell (Bio-Rad). The gels were stained for protein with Coomassie brilliant blue R-250 and for activity as described elsewhere [29].

2.8. Western blotting

After 12% SDS and 7.5% acrylamide native PAGE the mutant and the wild-type proteins were detected immunologically [30] using rabbit serum antibodies raised against the wild-type clostridial enzyme. The protein was transferred to a Hybond-C nitrocellulose membrane 0.45 μ m (Amersham) in a MiniProtean II trans-blot electrophoretic cell (Bio-Rad) for 1 hour. For immunodetection the filter was treated following the instructions of the amplified alkaline phosphatase Immuno-Blot kit (Bio-Rad).

2.9. Gel filtration chromatography

Superose 6 HR10/30 and Superose 12 (Pharmacia) pre-packed columns were used to estimate the apparent molecular weight under native conditions. The protein was loaded onto a column equilibrated with 50 mM phosphate buffer (pH 7) and 0.1 M NaCl at a constant flow rate of 0.5 ml/min on a Pharmacia FPLC system. Molecular weight marker proteins to calibrate the columns were: apoferritin (443 kDa), rabbit muscle aldolase (161 kDa), horse liver ADH (80 kDa), bovine serum albumin (66 kDa), chicken egg albumin (45 kDa) and cytochrome *c* (12 kDa).

2.10. Reaction with 5,5'-dithiobis(2-nitrobenzoic acid)

The enzyme (2 μ M final) was incubated in 0.1 phosphate buffer (pH 7) at 25°C in 1 ml final volume cuvette with 1 mM DTNB and the increase of absorbance at 412 nm due to the release of TNB⁻ was followed over 45 min [31,32].

2.11. Circular dichroism experiments

Near- and far-UV CD spectra of mutant and wild-type enzymes were recorded in a Jasco J600 spectropolarimeter. Cell path lengths were 0.1 and 1.0 cm for protein concentrations of 0.3 and 1.5 mg/ml, respectively, in 0.1 M phosphate buffer.

2.12. Analytical ultracentrifugation experiments

A Beckman Optima XL-A (Beckman, Spinco Division) analytical ultracentrifuge equipped with modern scanning absorption optics was used. The sedimentation velocity experiments were carried out at 20 000 and 25 000 rev/min and 20°C, whereas the sedimentation equilibrium experiments were performed at 7500 rev/min at the same temperature using 6-channel KEL-F centrepieces [33]. The sedimentation coefficients as well as the sedimentation equilibrium data were determined using the absorption optics of the Optima XL-A, scanning at 280 nm. All sedimentation coefficients were evaluated at least three times to minimize the errors resulting from the computer-graphical evaluation. The derived sedimentation coefficients in the buffer ($s_{T,b}$) were corrected to that at 20°C in water ($s_{20,w}$) using the following formula [34]:

$$\left(\frac{(1-\bar{v}\rho)_{20,w}}{(1-\bar{v}\rho)_{T,b}} \right) \left(\frac{\eta_{T,b}}{\eta_{20,w}} \right) s_{T,b} = F s_{T,b}$$

where \bar{v} is the partial specific volume of the polymer, ρ the solvent density, η the solvent viscosity and s the

Table 1

Buffer densities ρ , relative viscosities η and correction constants F of the biopolymer in the appropriate buffer at 20°C (wild-type in phosphate buffer, F187D in the same buffer + 1 mM EDTA)

	ρ (g/ml)	η	F
Phosphate buffer	1.00792	1.0065	1.0322
Phosphate buffer + EDTA	1.00435	1.0047	1.0200

sedimentation coefficient with the indices w for water, b for buffer and T for temperature. The partial specific volumes of the proteins were calculated from their amino-acid compositions giving, $v = 0.7359$ ml/g for the wild type and 0.7355 ml/g for F187D. The molar mass of the wild-type monomer was calculated to be 49 295 g/mol and that of the F187D monomer to be 49 261 g/mol.

For the evaluation of the sedimentation equilibrium data the MSTAR program [35] was used (Cölfen, H. and Harding, S.E. in preparation).

The buffer densities were determined at 20°C using a precision density meter (Anton paar DMA 02C) according to the method of Kratky [36]. For the determination of the buffer viscosities at 20°C, an automatic viscometer (Schott Geräte AVS 310) was applied. For the density as well as for the viscosity 10 readings were taken to minimise the experimental error. The buffer densities ρ , the relative viscosities η and the correction constants F of the biopolymer in the appropriate buffer (wild-type in 0.1 M phosphate buffer pH 7, F187D same buffer plus 1 mM EDTA) are listed in Table 1.

3. Results and discussion

Construction of the mutant gene was achieved by annealing a synthetic oligonucleotide carrying a two-base change into the DNA. This converted a TTC Phe codon into GAC coding for Asp. Mutagenesis was carried out as described in the experimental procedure and the entire *gdh* gene was checked for secondary and undesired mutations by sequencing.

The expression of the mutant enzyme was carried out after transformation of *E. coli* strain PA340 with the expression vector ptac 44-F187D grown overnight at 37°C in Luria-Bertani medium supplemented with 0.1 mg/ml ampicillin and induced with 0.5 mM final concentration of IPTG.

The mutant enzyme was purified to near homogeneity (Fig. 3A) but showed no detectable activity in the standard forward and reverse assays with up to 60 μ g F187D protein per 1 ml. assay. Screening with antibodies to native GDH was therefore necessary to monitor and confirm

purification. Fig. 3B shows Western blotting of F187D transferred to nitrocellulose after denaturing gel electrophoresis in comparison with wild-type GDH. This indicates production of a cross-reacting protein with the correct subunit M_r . Different behaviour of the mutant enzyme and wild-type in non-denaturing electrophoresis, however, indicated that the two enzymes have different size and/or surface charge (data not shown).

The molecular weight of the mutant enzyme was checked on a Superose 12 HR 10/30 pre-packed column calibrated with appropriate standards and the apparent molecular weight calculated for the elution volumes gave a M_r of 87 ± 3 kDa (data not shown).

The changed chromatographic behaviour of the mutant enzyme with respect to the dye-ligand Remazol red raised the suspicion that the lack of activity might reflect major misfolding and possibly loss of the ability to bind the coenzyme (on the assumption that the dye has an affinity for the coenzyme binding site in the wild-type enzyme).

DTNB modification experiments on the wild-type enzyme have shown that, of the two cysteine residues per subunit (C320 and C144), only C320 is modified by this reagent [6,31,37]. The same experiment for F187D showed a stoichiometry of modification of 2.0 cysteine residues per subunit. At first sight this result is somewhat surprising since crystallographic studies have shown that the residue C144 is buried even in the monomer. However, in the hexamer the N-terminal domains are tightly packed against

one another across the dimer interface, and thus in the trimer removal of this stabilisation may change the dynamic properties of this molecule and result in exposure of this residue to solvent during the course of its normal modes of vibration. Thus, to some extent at least, this mutant does behave as if some structural perturbation of individual subunits has occurred. This is further confirmed by the different behaviour in protection experiments. Whilst the wild-type enzyme shows complete protection of the single modifiable cysteine from DTNB modification in the presence of 1 mM NAD^+ [37], in the mutant enzyme only one of the two cysteines, presumably C320, is protected by the coenzyme. This result suggests, nevertheless, that the mutant enzyme binds NAD^+ normally.

Far-UV CD spectra of the wild-type and mutant enzymes adjusted for protein concentration show the same secondary structure and moreover that the mutant enzyme has a similar fold to that of the native enzyme (Fig. 4A). The near-UV region (Fig. 4B), however, shows a less intense signal compared to the wild-type, and the two shoulders at 262 and 268 nm respectively indicate strong Phe contribution. One possible origin for this difference may be that in the dimer the side chain of Phe 199, which occurs in the loop between β_f and α_g , would be expected to be almost completely exposed to the solvent.

Ultracentrifugation experiments showed quite well-defined sedimenting boundaries for the wild-type (Fig. 5A) and also for F187D (Fig. 5B). This indicates good prepara-

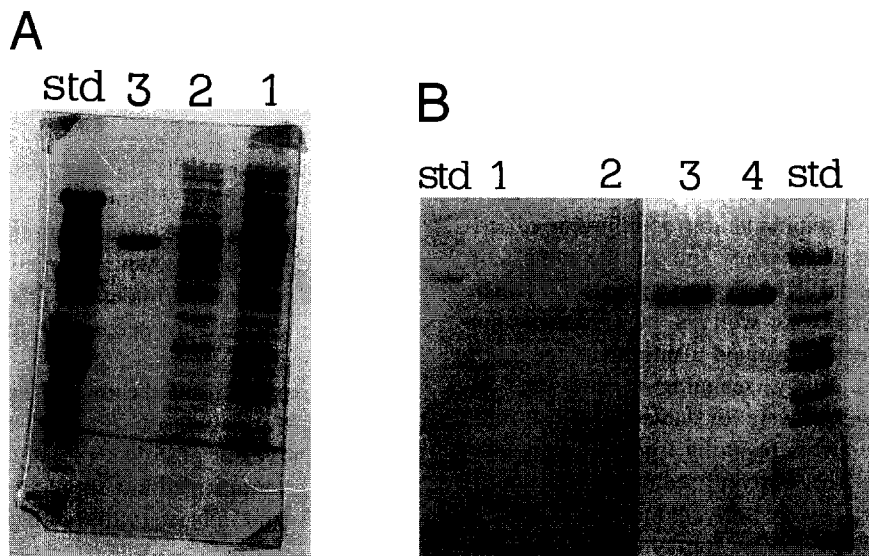


Fig. 3. SDS-PAGE electrophoresis of wild-type and mutant enzyme stained with Coomassie brilliant blue R250. (A) Lane 1, crude extract of *E. coli* expressing F187D GDH; lane 2, 40–60% ammonium sulfate fraction; lane 3, purified F187D GDH; Std, low molecular weight standards (Bio-Rad). (B) Left panel: Western blotting after SDS-PAGE detected with antibodies; lane 1, F187D GDH; lane 2, wild-type GDH; Std, prestained low molecular weight standard (Bio-Rad). Right side of the photo shows the counterpart stained with Coomassie brilliant blue R250; lane 3: wild-type GDH; lane 4: F187D GDH.

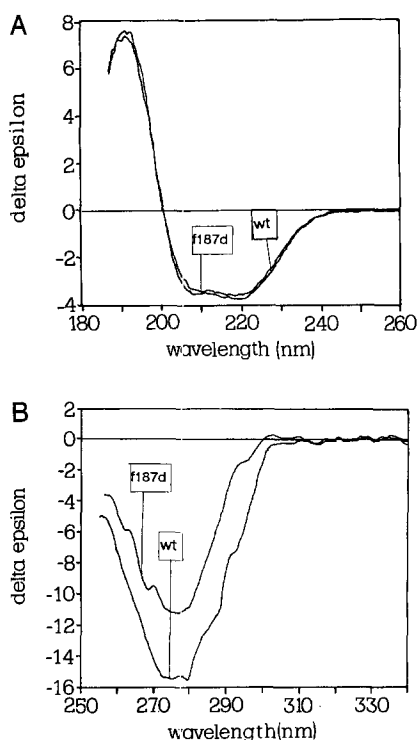


Fig. 4. Circular dichroism spectra. Far-UV (A) and near-UV (B) spectra for the wild-type (wt) and the mutant (F187D) GDH. Spectra of the two enzymes were corrected for protein concentration (1.2 mg/ml) and recorded in 0.1 M phosphate buffer (pH 7).

tions without significant impurities. The boundary for F187D is much more spread owing to diffusion, as expected for a smaller relative molecular mass species.

The corrected sedimentation coefficients $s_{20,w}$ were respectively 11.08 S and 5.29 S for the wild-type (2.48 mg/ml) and mutant enzyme (1.09 mg/ml). Comparing these two results with the gel filtration data, the sedimentation coefficient of 11 S corresponds to the hexameric form, whereas the value of 5.3 S indicates a dimer or possibly another dissociation product, depending on the conformation which is not known.

To obtain more definitive estimates of molecular mass, more quantitative information was sought through sedimentation equilibrium experiments. These gave a weight average molar mass $M_{w,app}$ of $280\,000 \pm 5\,000$ g/mol for the wild-type, which clearly indicates the hexamer. The value of $135\,000 \pm 3\,000$ g/mol at 1.09 mg/ml lies between those for a dimer (99 000) and a trimer (148 000). As only a single sedimenting component could be observed in the sedimentation velocity profile (Fig. 5B), this result hints either at polydispersity or at rapid self-association. To investigate this further, equilibrium experiments were performed with F187D samples at different concen-

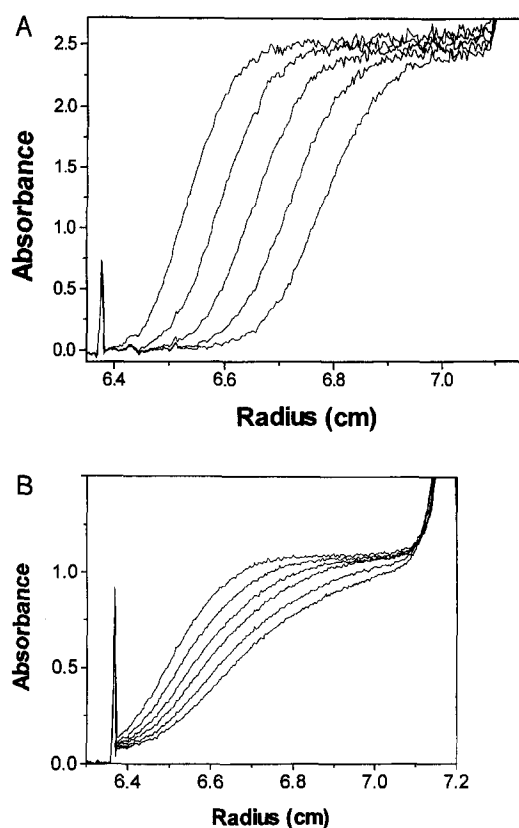


Fig. 5. Analytical ultracentrifuge diagrams. Spectrophotometric sedimentation velocity patterns for the wild-type (A) and F187D (B) mutant GDH in phosphate buffer at 20°C, respectively, at 20 000 and 25 000 rpm. The scan interval between the scans is 20 min. For clarity, not all scans have been included.

trations (0.1–2.0 mg/ml). As can be seen in Fig. 6, the concentration dependence is linear, obeying the regression equation: $M_{w,app} = 108\,118.5 \text{ g/mol} + 25\,019 \text{ l/mol C}$

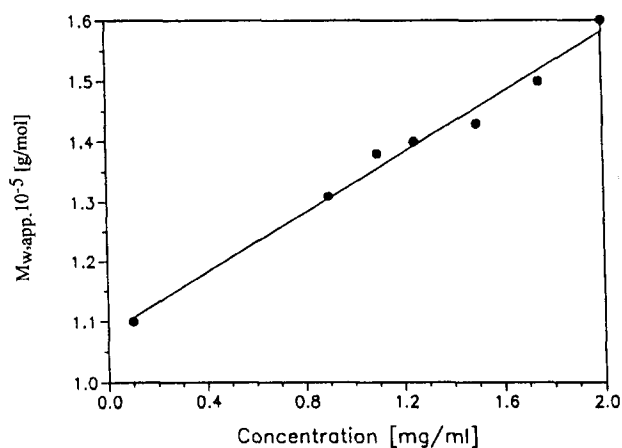


Fig. 6. Plot of $M_{w,app}$ vs. loading concentration of F187D.

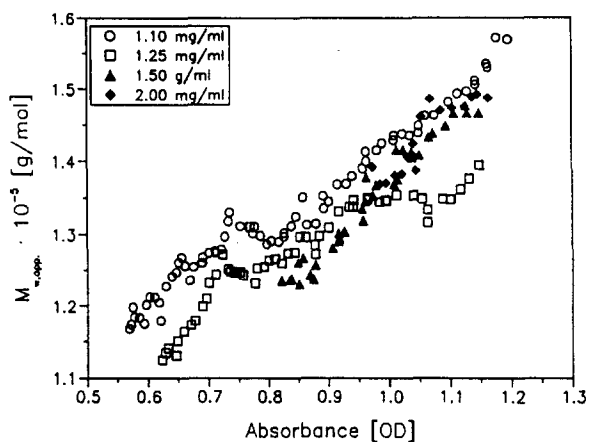


Fig. 7. Plot of $M_{w,app}$ vs. concentration of F187D in absorbance units for different initial concentrations. These data have been derived from the local slopes of the $\ln A$ vs. r^2 plots using the MSTAR program 35.

(concentration in g/l). This gives an M_w of 108 118 g/mol at infinite dilution, in reasonably good agreement with the expected value for a dimer. The value calculated for the 1.09 mg/ml sample using this equation is 135 390 g/mol in good agreement with the observed $M_{w,app}$. Therefore Fig. 6 indicates self-association, with the dimer being the smallest species. As a rapid equilibrium between dimer and trimer is most unlikely, and furthermore not supported by Fig. 6 where $M_{w,app}$ for the 2 mg/ml sample already is $160\,000 \pm 4000$ g/mol, three dimers presumably associate to form a hexamer. This must then be a rapid equilibrium, because the sedimentation velocity data clearly indicate a single sedimenting species.

To distinguish clearly between polydispersity and self-association, there exist several diagnostic plots. One applies the coincidence of the so called Omega functions for different samples but equal reference concentrations in the case of a self associating sample [38]. Another approach is to plot $M_{w,app}$ versus the concentration for samples with different initial concentrations [39,40]. Plots of local $M_{w,app}$ coincide in the case of self-association but they do not for a polydisperse sample. The results for some different initial concentrations of F187D are presented in Fig. 7. The data are relatively noisy and needed smoothing as the slopes in plots of $\ln A$ vs. r^2 are very sensitive to experimental noise. However, it can be seen that the curves in Fig. 7 coincide within the relatively large error of such $M_{w,app}(r)$ values derived via the local slopes in the $\ln A$ vs. r^2 plots. Together with the information from Figs. 6 and 7 that $M_{w,app}$ increases with concentration, this allows a confident conclusion that the mutant enzyme undergoes a self-association reaction. Using the dimer–hexamer equilibrium and the $M_{w,app}$ values in Fig. 6, a relationship for a

thermodynamically ideal association governed by a single equilibrium constant can be applied [41].

$$\left(\frac{M_w}{M_1}\right)^2 - 1 = 4kc$$

where M_1 is the molar mass of the monomer, M_w the weight-average molar mass, c the polymer concentration and k the isodesmic self-association constant. Applying the binomial theorem, the above equation may be written as:

$$M_w = M_1 + 2kM_1c + \dots$$

Using the above-derived value of 25 019 l/mol for $2kM_1$, an equilibrium constant of 0.13 l/g can be calculated if M_1 is taken as 98 522 g/mol (dimer). This indicates a weak dimer–hexamer association.

As an independent check of the equilibrium constant, a non-linear least squares analysis has been applied to the experimental raw data (radial absorption scans) using the self-association model for an ideal species and multiple data sets implemented into the Microcal Origin software [39]. In this model, the molar mass of the smallest associating species (dimer), the baseline absorbance, the stoichiometry of the reaction and the equilibrium constant were allowed to vary. The baseline absorbances calculated were very close to those determined experimentally by meniscus depletion. The molar mass of the smallest associating species came out to be 108 820 g/mol, in very good agreement with the value derived from Fig. 6. The stoichiometry of the reaction was determined to be three, which confirms the dimer–hexamer association, as the smallest associating species is the dimer. The self-association constant is 0.11 l/g, also in good agreement with the value derived earlier. To test whether the experimental curves are properly described by a dimer–hexamer self-association using the above given dataset, the simulated curves for given initial loading concentrations of F187D were compared to the experimentally determined ones. The residuals were calculated and should be statistically distributed around 0. Representative plots are shown in Fig. 8A, B and those for other concentrations were of similar quality, although there were slight systematic deviations in the residual plots for the 1.1 mg/ml sample and the 1.25 mg/ml sample. The selected model for a dimer–hexamer self-association with an equilibrium constant of 0.11 l/g describes the sedimentation equilibrium results for F187D well especially if it is taken into account that 7 experimental equilibrium curves for different initial concentrations are nicely fitted without major deviations. Hence the model and the derived parameters can be treated as reliable. This is furthermore supported by the good agreement with the data derived independently from Fig. 6.

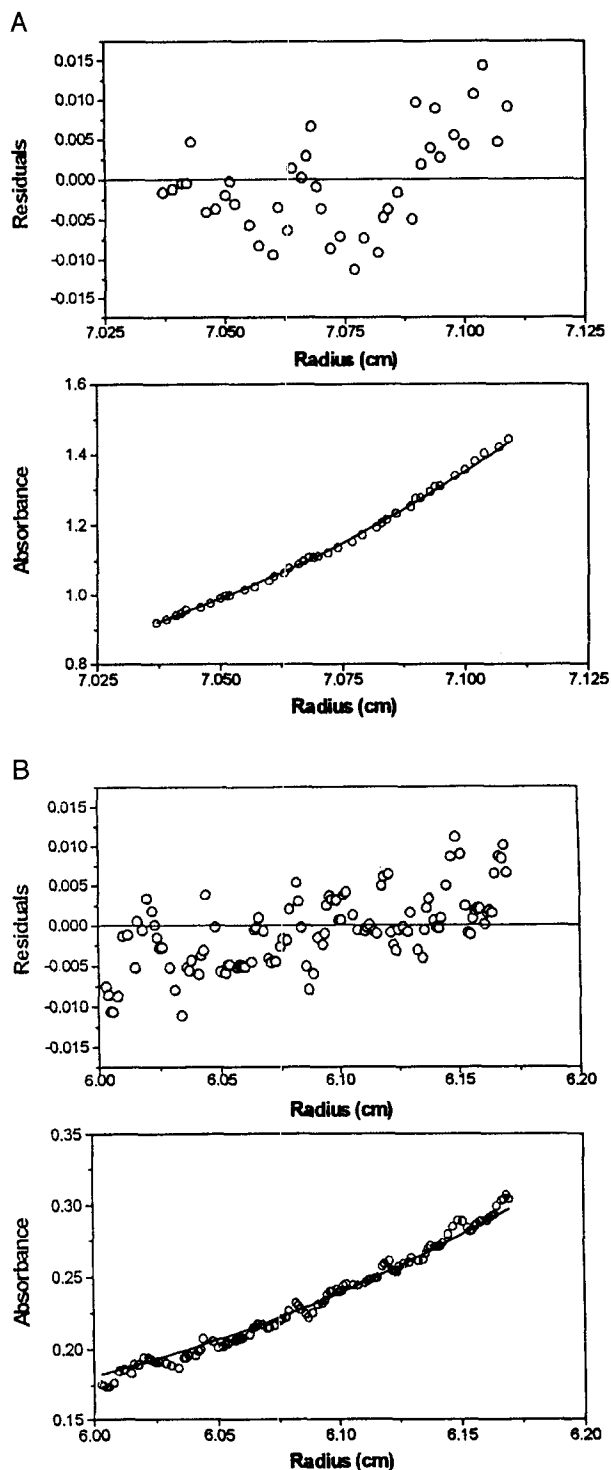


Fig. 8. Plots of simulated equilibrium concentration gradient of F187D enzyme in absorbance units (solid line in the lower part of the figure) with the experimental curve (open circles in the lower half of the figure). The residuals are given in the upper half of the plot. The samples were at loading concentration of 0.1 mg/ml (A), 2.0 mg/ml (B).

The targeted mutation of F187D appears to have been sufficient to destabilise the hexameric structure and produce a form of GDH that is predominantly dimeric. The general similarity of the circular dichroism signal indicates that the mutant enzyme is essentially correctly folded. The recent crystallisation of the mutant, (unpublished results) and the demonstration of NAD^+ binding also both support the view that it is structurally intact. Although the near-UV CD does show an alteration of the environment of aromatic residues, none have so far been implicated as key contributors to catalytic activity. However, the different reactivity towards DTNB and the loss of a strong affinity for Remazol red resin are undoubtedly indicative of some structural changes which are evident in the far-UV CD. One question that therefore arises is whether the lack of activity is an inevitable result of the change in quaternary structure or whether perhaps it reflects some other damaging and specific consequences of the chosen mutation. Previous studies [20] have highlighted the importance of a major domain arrangement which is thought to occur during the enzyme's catalytic cycle. Furthermore, recent work on the structure determination of the *E. coli* GDH [42] has shown how contacts across the three-fold interface can influence the domain conformation. Thus, for correct GDH function, it is clear that the dynamic properties of the molecule are essential. This specific dimer could be inactive for reasons associated with a subtle disruption of its tertiary rather than quaternary structure. In such a case the corresponding hexamer, if formed, would also be inactive. Although the hexameric form of this mutant enzyme is indeed formed to some extent at high protein concentration, its contribution would be negligible even at the highest concentration used for catalytic assay in this study. It thus remains possible, though not proven, that F187D GDH is inactive because it is dimeric. Further information, both from the structure of this mutant and from the analysis of the properties of other mutations which destabilise this and other subunit interfaces, should clarify the role of the quaternary structure in enzyme function.

Acknowledgements

We are grateful to Drs R. Chiaraluce and V. Consalvi for scientific discussion, and to Dr C.B. Taylor for raising antibodies against clostridial GDH. A.P. is supported by Italian MURST. This project is supported by the EC Biotechnology Program. The Krebs Institute is a designated Biomolecular Sciences Centre of the U.K. Biotechnology and Biological Sciences Research Council.

References

- [1] Smith, E.L., Austen, B.M., Blumenthal, K.M. and Nyc, J.F. (1975) *The Enzymes*, 3rd Ed. (Boyer, P.D., ed.), Vol. 11, pp. 293–367, Academic Press, New York.
- [2] Britton K.L., Baker, J.P., Rice, D.W. and Stillman, T.J. (1992) *Eur. J. Biochem.* 209, 851–859.
- [3] Rice, D.W., Baker, P.J., Farrants, G.W. and Hornby, D.P. (1987) *Biochem. J.* 242, 789–795.
- [4] Dean, J.L.E., Wang, X.G., Teller, J.K., Waugh, M.L., Britton, K.L., Baker, P.J., Stillman, T.J., Martin, S.R., Rice, D.W. and Engel, P.C. (1994) *Biochem. J.* 301, 13–16.
- [5] Syed, S.E., Engel, P.C. and Parker, D.M. (1991) *Biochim. Biophys. Acta* 1115, 123–130.
- [6] Basso, L.A. and Engel, P.C. (1994) *Biochim. Biophys. Acta* 120, 222–226.
- [7] Baker, P.J., Britton, K.L., Engel, P.C., Farrants, G.W., Lilley, K.S., Rice, D.W. and Stillman, T.J. (1992) *Proteins* 12, 75–86.
- [8] Goldin, B.R. and Frieden, C. (1971) *Curr. Top. Cell Regul.* 4, 77–117.
- [9] Fisher, H.F. (1973) *Adv. Enzymol.* 39, 369–417.
- [10] Bell, E.T. and Bell, J.E. (1984) *Biochem. J.* 217, 327–330.
- [11] Karabashian, L.V., Aghajanian, S.A., Danoyan, K.V. and Kazarian, R.A. (1989) *Bioorgan. Khimiya* 15, 32–39.
- [12] Karabashian, L.V., Aghajanian, S.A., Danoyan, K.V. and Kazarian, R.A. (1988) *Bioorgan. Khimiya* 14, 1502–1508.
- [13] Karabashian, L.V., Aghajanian, S.A., Danoyan, K.V. and Kazarian, R.A. (1988) *Bioorgan. Khimiya* 14, 1495–1501.
- [14] Consalvi, V., Chiaraluca, R., Politi, L., Gambacorta A., De Rosa, M. and Scandurra, R. (1991) *Eur. J. Biochem.* 196, 459–467.
- [15] Consalvi, V., Chiaraluca R., Millevoi, S., Pasquo, A., Politi, L., De Rosa, M. and Scandurra, R. (1994) *Comp. Biochem. Physiol.* 109B, 691–699.
- [16] Teller, J.K., Smith, R.J., McPherson, M.J., Engel, P.C. and Guest, J.R. (1992) *Eur. J. Biochem.* 206, 151–159.
- [17] Baker, P.J., Britton, K.L., Rice, D.W., Rob, A. and Stillman, T.J. (1992) *J. Mol. Biol.* 228, 662–671.
- [18] Rossmann, M.G., Moras, D. and Olsen, K.W. (1974) *Nature* 250, 94–199.
- [19] Rossmann, M.G., Liljas, A., Brändén, C.I. and Banaszak, L.J. (1975) *The Enzymes*, 3rd Ed. (Boyer, P.D., ed.), Vol. 11, pp. 61–102, Academic Press, New York.
- [20] Stillman, T.J., Baker, P.J., Britton, K.L. and Rice, D.W. (1993) *J. Mol. Biol.* 234, 1131–1139.
- [21] Lilley, K.S., Baker, P.J., Britton, K.L., Stillman, T.J., Brown, P.E., Moir, A.G., Engel, P.C., Rice, D.W., Bell, J.E. and Bell, E. (1991) *Biochim. Biophys. Acta* 1080, 191–197.
- [22] Marsh, P. (1986) *Nucleic Acid Res.* 14, 3603.
- [23] Sambrook, J., Fritsch, E.F. and Maniatis, T. (1989). *Molecular Cloning. A Laboratory Manual*, 2nd Ed., Cold Spring Harbor Laboratory Press, Cold Spring Harbor, NY.
- [24] Wieslander, L. (1979) *Anal. Biochem.* 98, 305–309.
- [25] Kunkel, T.A., Roberts, J.D. and Zakour, R.A. (1987) *Methods Enzymol.* 154, 367–382.
- [26] Sanger, F., Nicklen, S. and Coulson, A.R. (1977) *Proc. Natl. Acad. Sci. USA* 74, 5463–5467.
- [27] Syed, S.E.-H. (1987) *Doctoral Thesis*, University of Sheffield.
- [28] Laemmli, U.K. (1970) *Nature* 227, 680–685.
- [29] Wang, X.G. and Engel, P.C. (1994) *Protein Eng.* 8, 147–152.
- [30] Harlow, E. and Lane, D. (1988) *Antibodies: A Laboratory Manual*, Cold Spring Harbour Laboratory Press, Cold Spring Harbor, NY.
- [31] Syed, S.E.-H., Hornby, D.P., Brown, P.E., Fitton, J.E. and Engel, P.C. (1994) *Biochem. J.* 298, 107–113.
- [32] Ellman, G.L. (1959) *Arch. Biochem. Biophys.* 74, 443–450.
- [33] Creeth, J.M. and Harding, S.E. (1982) *J. Biochem. Biophys. Methods* 8, 25–34.
- [34] Tanford, C. (1961) *Physical Chemistry of Macromolecules*, Wiley, New York.
- [35] Harding, S.E., Horton, J.C. and Morgan P.J. (1992) *Analytical Ultracentrifugation in Biochemistry and Polymer Science* (Harding, S.E., Rowe, A.J. and Horton, J.C., eds.), p. 275, Royal Society of Chemistry, Cambridge.
- [36] Kratky, O., Leopold, H. and Stabinger, H. (1973) *Methods Enzymol.* 27, 98–110.
- [37] Wang, X.G. and Engel, P.C. (1994) *Protein Eng.* 7, 1013–1016.
- [38] Milthorpe, B.K., Jeffrey, P.D. and Nichol, L.W. (1975) *Biophys. Chem.* 3, 169.
- [39] McRorie, D.K. and Voelker, P.J. (1993) *Self-Associating Systems in the Analytical Ultracentrifuge*, Beckman Instruments, Inc., Palo Alto, CA.
- [40] Laue, T.M. (1992) *Short Column Sedimentation Equilibrium Analysis for Rapid Characterization of Macromolecules in Solution*. Technical Information DS-835, Beckman Spinco Business Unit, Palo Alto, CA.
- [41] Van Holde, K.E., Rosetti, G.P., Dyson, R.D. (1969) *Ann. N.Y. Acad. Sci.* 164, 279.
- [42] Abeyasinghe, I.S.B. (1993) *Doctoral Thesis* University of Sheffield.